AN ANALYSIS OF TEMPERATURE-INDUCED ERRORS FOR AN ULTRASOUND DISTANCE MEASURING SYSTEM

NAGW-1333

by

David Paul Wenger

Rensselaer Polytechnic Institute
Electrical, Computer, and Systems Engineering Department
Troy, New York 12180-3590

December 1991

CIRSSE REPORT #106

AN ANALYSIS OF TEMPERATURE-INDUCED ERRORS FOR AN ULTRASOUND DISTANCE MEASURING SYSTEM

by

David Paul Wenger

A Thesis Submitted to the Graduate
Faculty of Rensselaer Polytechnic Institute
in Partial Fulfillment of the
Requirements for the Degree of
MASTER OF SCIENCE

Approved:

_____

Dr. Robert B. Kelley
Thesis Advisor

Rensselaer Polytechnic Institute
Troy, New York

December 1991

CONTENTS

LIST OF TABLES

LIST OF FIGURES

ACKNOWLEDGMENTS

As I complete my work on this project and review the past year spent on it I begin realize the number of people who have supported me in so many ways. I would first like to thank Dr. Robert Kelley for his guidance and analytical technique which led me to this project and taught me the importance of thoroughness. I also want to thank Andrew Silverthorne for his interest in the work and his willingness to go out of his way to help collect the ultrasound data. I would also like to thank my very good friends Keith Fitch and Brian Mitchell who both played key roles in motivating me to continue on with graduate studies. Additionally, I give my thanks and love to my entire family who, throughout my life, have encouraged me to be the best I can; especially my parents who, through their own lives, have taught me to respect, as well as utilize to its fullest, the mind which God has given me. Finally, I need to express my fullest and sincerest love to my wife, Monica, who was so giving, supportive, and understanding through it all.

CHAPTER 1
INTRODUCTION

Motivation

As an aid to the Center for Intelligent Robotic Systems for Space Exploration's (CIRSSE's) dual PUMA 560 robot arm testbed at Rensselaer, research concerning the amount of error in ultrasound distance measurements has been carried out to enable further research and design of an arm collision avoidance system. An external collision avoidance system, which does not depend on internal arm location data from encoders, provides a redundant method for determining arm locations and therefore a more reliable method for avoiding collisions.

Using a time-of-flight method for measuring the distances between ultrasonic transducers mounted on the robot arms, the 3-space location of those transducers, and hence, the distance between the arms can be determined. Determining the bounds of the error in the distance measurements enables the determination of how accurately the 3-space locations on the arms can be known, and therefore how efficiently and exactly a collision avoidance system can determine if a collision will occur.

General Problem Solution

Determining the 3-space location of the arm joints in the testbed can be accomplished through the use of ultrasonic transducers. Each arm joint of interest has a transmitting unit associated with it which transmits an

ultrasonic tone burst. The tone burst is received by a grouping of ultrasonic microphone receivers set up in a known configuration. Based on the time during which the tone burst travels from the transmitter to the receiver, a slant range can be determined by the simple relation D = ct where D is the slant range between the transmitter and receiver, c is the speed of the sound wave in air, and t is the time of flight necessary for the received tone burst to travel from the transmitter to a given receiver.

Using a 3-space Cartesian coordinate system a minimum of three slant range measurements are required to determine each 3-space location. For the most basic collision avoidance system, at least two sets of measurements, each taken with respect to a given point on each arm, are required. Finding the distance between these two points determines the proximity of the arms and can alert a collision avoidance system should the distance fall below a predetermined threshold. More accurate and robust collision avoidance can be accomplished by placing an individual transmitter at additional points of interest on each arm. Determining the 3-space locations of these additional points of interest, and taking the distances between these points provides better knowledge of the location of each arm with respect to the other and allows a more accurate collision avoidance system to be developed.

In order to avoid time- and/or frequency-multiplexing issues, and as the main intent of this research is to determine error bounds on the accuracy of ultrasonic 3-space measurements, emphasis is placed on accurately obtaining only one set of slant ranges. An ability to determine the upper bound on the measurement error leads to the formulation of methods to minimize the inaccuracy of ultrasonic distance measurements. The results of this work can then be extended to the design of a fully functional collision

avoidance system which accurately obtains multiple sets of slant ranges for a more accurate determination of collision danger.

Outline of Thesis

The presentation of research is provided in the following five chapters. Chapter 2 presents the necessary background information and definitions for general work with ultrasound and acoustics. It also discusses the basis for errors in the slant range measurements. Chapter 3 presents a method of problem solution and an analysis of the sensitivity of the equations to slant range measurement errors. It also presents various methods by which the error in the slant range measurements can be reduced to improve overall measurement accuracy. Chapter 4 provides a description of a type of experiment used to test the analytical solution and provides a discussion of its results. Chapter 5 discusses the setup of a prototype collision avoidance system, discusses its accuracy, and demonstrates various methods of improving the accuracy along with the improvements' ramifications. Finally, Chapter 6 provides a summary of the work and a discussion of conclusions drawn from it. Additionally, suggestions for further research are made to improve upon what has been presented here.

CHAPTER 2
BACKGROUND

Ultrasound

In order to accurately measure distances for the problem at hand, using non-mechanical measurement methods, the simple time of flight principle is utilized

$$D = ct \tag{2.1}$$

where t is the time necessary for a wave traveling at speed c to traverse a distance D.

Several options exist for the design of a non-mechanical measurement system, and depend solely on the type of wave chosen to be emitted to measure its time of flight. One option is to use wave emissions in the electro-optical spectrum; however, since they travel at the speed of light, 2.1 shows that their time of flight over short distances where $c \approx 3 \times 10^8$ m/s will be on the order of 10^{-12} seconds for mm accuracy and may be difficult to measure accurately. On the other hand, if acoustic waves are used, which travel at the speed of sound ($c \approx 340$ m/s), the time of flight measurements are easier to make as they require timing accuracy on the order of 10^{-6} seconds for mm accuracy.

Acoustic waves consist of both audible and inaudible frequencies. The human ear is only able to detect sounds in the frequency range of approximately 20 Hz to 20,000 Hz; humanly inaudible frequencies emitted above 20 KHz are defined as ultrasonic frequencies. Ultrasound is a useful

tool for measuring distances mainly because its frequencies allow time of flight measurements to be made more easily than electro-optical frequencies, and also because of its insusceptibility to ambient noise within its acoustic environment. This study proposes to determine how accurately ultrasound can be used to compute distances via the time of flight measurement method. While multiple factors affect the propagation of a sound wave through a given medium, emphasis is placed on those factors which most directly limit the accuracy of ultrasound-based distance measurements.

Speed of Sound in a Medium

The expression for the speed of sound in air is commonly given as

$$c = (ß / \rho)^{1/2} \tag{2.2}$$

where ρ is the density of the medium, and ß is the adiabatic bulk modulus of the medium[1]. ß is defined as:

$$ß = (\gamma - 0.1e)\, P \tag{2.3}$$

where γ is the ratio of specific heats (1.402 in air) and e is the vapor pressure within the medium[1][2].

The speed of sound depends on many factors. Changes in temperature, relative humidity, and pressure all affect the speed of sound within an environment. For the purposes of this study, pressure changes will not be studied as the assumption is made that pressure is constant throughout the medium and therefore induces no changes in the speed of sound.

Changes in the speed of sound due to changes in the medium's temperature arise from the following interpretation of equations 2.2 and 2.3.

The relation for ρ which states that

$$\rho = \rho_0 \frac{273}{K} \frac{P}{P_0} \tag{2.4}$$

where ρ and ρ_0 are the instantaneous and constant equilibrium densities of the medium; K is the temperature of the medium in °K; and P and P_0 are the instantaneous and constant equilibrium pressures of the medium shows that 2.2 can be rewritten as

$$c = \left(\frac{\beta}{\rho_0} \frac{K}{273} \frac{P_0}{P} \right)^{1/2} \tag{2.5}$$

Equation 2.5 then reduces to

$$c = c_0 \frac{(T + 273)^{1/2}}{(273)^{1/2}} \tag{2.6}$$

after noting that K can be written as T + 273, where T is the temperature of the environment in °C, and c_0 is the speed of sound in air at 0°C.

Humidity plays a role in changing the speed of sound within a medium. Changes in the speed of sound due to changes in the medium's humidity arise from another interpretation of equations 2.2 and 2.3.

Substituting 2.3 into 2.2 gives

$$c = \frac{((\gamma - 0.1e) P)^{1/2}}{\rho^{1/2}} \tag{2.7}$$

Changes due to humidity directly affect the vapor pressure, e, which, in turn, affect the speed of sound. The relation between humidity and vapor pressure is given as

$$H\ (\%) = (100\%)\ \left(\frac{Pp}{e}\right) \tag{2.8}$$

where H is the relative humidity, Pp is the partial pressure of the water vapor in the medium, and e is the vapor pressure at the same temperature [3]. The relation between Pp and e is such that at any given temperature

$$0 < Pp < e.$$

Knowing this relation enables a substitution of Pp for e in equation 2.7. Table 2.1 shows a partial listing of measured vapor pressures for water at different temperatures.

T (°C)	e (10^5 Pa)
0.0	0.00610
5.0	0.00868
10.0	0.0119
15.0	0.0169
20.0	0.0233
40.0	0.0734

Table 2.1 — Vapor Pressure of Water

Holding all other factors constant and varying Pp from [0, e] allows an examination of how c changes with Pp over the given range. From the

values listed in Table 2.1 it is obvious that in the temperature range of interest, [15°C, 25°C], contributions of Pp are minimal and the 0.1e term can be neglected; thus reducing equation 2.7 to the results of 2.6. This means that changes in c depend much more on changes in temperature than on changes in humidity. Additionally, the changes in c due to its dependency on temperature means that many temperature changes along the acoustic wave's path will affect the speed of the wave at many points from emission to detection and will require finding ways of handling the error-inducing temperature gradients.

Further information concerning the derivations of the speed of sound within a given medium, and the effects of a dynamic environment on that speed can be found in references [1] to [9].

CHAPTER 3
SOLUTION AND ANALYSIS

Problem Solution

The solution to the collision avoidance problem requires accurate determination of a specific point in 3-space using ultrasonic distance measurements (slant ranges). While a minimum of three slant ranges is required to determine the 3-space location in a Cartesian coordinate system, a fourth slant range is included in this analysis. The additional slant range is not necessary to solve the system; however, its addition reduces the number of variables in the expression of one of the 3-space location components (D_Z for example) to fewer than the number of variables in the expression for D_Z which is not based on the additional slant range measurement. A reduction in the number of variables in the expression reduces the number of variables in the corresponding derivative expression, thereby simplifying the analysis of error propagation in that 3-space location component.

Figure 3.1 demonstrates the geometrical setup of the solution. The location of the ultrasonic transducer source is given at point S along the Z axis of the coordinate system. The ultrasonic receivers are located at points P_1 through P_4. The distances between the transducer and the ultrasonic receivers are given by L_1 through L_4. Finally, the distances d_{12}, d_{23}, and d_{24} indicate the known distances between the receiver points P_1 and P_2, P_2 and P_3, and P_2 and P_4 respectively. The distances D_X, D_Y, and D_Z are the X, Y, and Z components of S's displacement from point P_1, which can be found as shown.

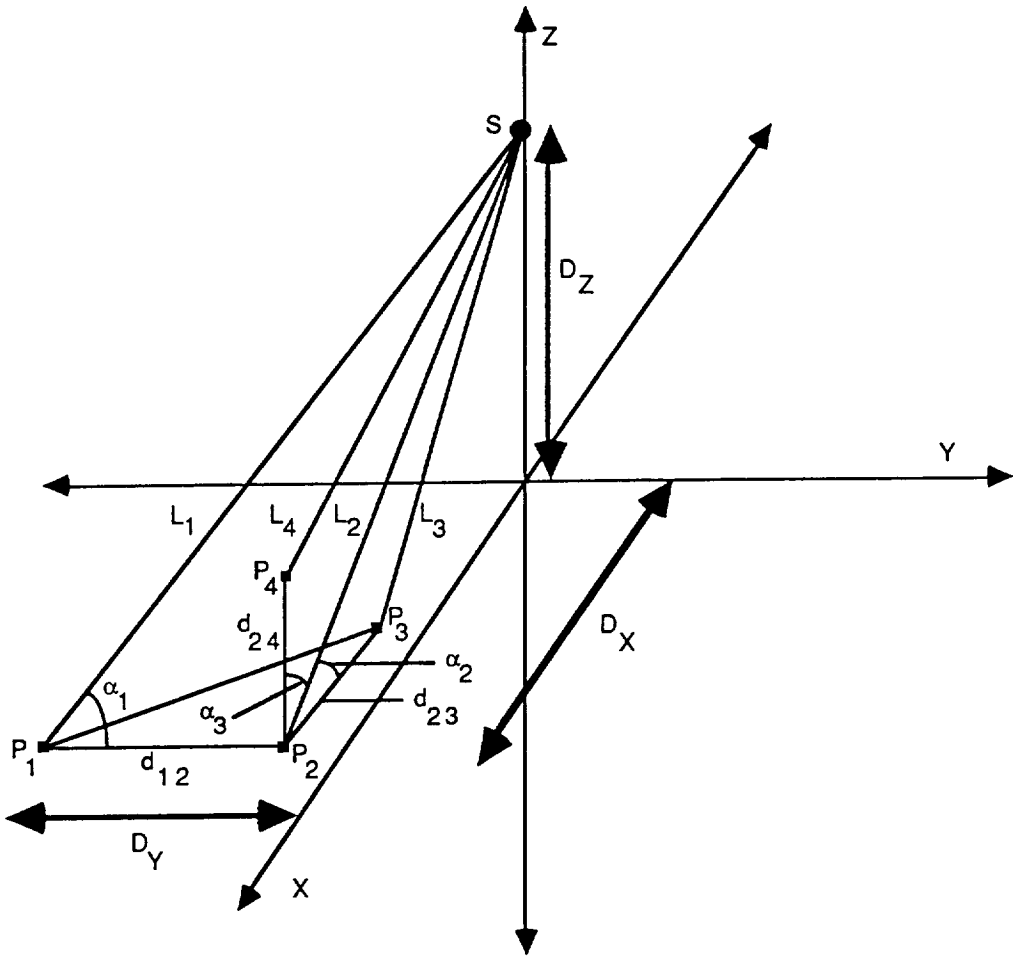

Figure 3.1 — Geometrical Setup of Solution

From Figure 3.1, D_X can be determined from the relationship:

$$D_X = L_2 \cos \alpha_2 \tag{3.1}$$

additionally, by the law of cosines:

$$\cos \alpha_2 = \frac{L_2^2 + d_{23}^2 - L_3^2}{2\, L_2\, d_{23}} \tag{3.2}$$

so that D_X can be found as:

$$D_X = \frac{L_2^2 + d_{23}^2 - L_3^2}{2\, d_{23}} \tag{3.3}$$

In the same manner, similar equations for both D_Y and D_Z can be found as:

$$D_Y = L_1 \cos \alpha_1 \tag{3.4}$$

and

$$D_Z = L_2 \cos \alpha_3 \tag{3.5}$$

These equations further reduce to:

$$D_Y = \frac{L_1^2 + d_{12}^2 - L_2^2}{2\, d_{12}} \tag{3.6}$$

and

$$D_Z = \frac{L_2^2 + d_{24}^2 - L_4^2}{2\, d_{24}} \tag{3.7}$$

Sensitivity Analysis of Solution

The accuracy of all of the distance equations above depends solely on the accuracy with which the slant ranges are measured. The use of the relation D = ct implies that the slant range measurement errors will occur due to errors in the measurements of sound velocity or flight time. In practical use, the flight time measurement error is minimal and can be ignored. The speed of sound, however is subject to more substantial measurement errors since it varies with any temperature changes along the acoustic wave's path.

Recall that from previous work in Chapter 2

$$c = c_0 \frac{(T + 273)^{1/2}}{(273)^{1/2}} \tag{3.8}$$

where c_0 is the velocity of sound in air at 0 °C; that is $c_0 \approx 331.18$ m/s.

Taking the derivative of 3.8 gives the change in speed of sound due to the change in temperature of the environment as:

$$dc = \frac{c_0}{2} \frac{(273)^{1/2}}{(T + 273)^{1/2}} \frac{dT}{273} \tag{3.9}$$

If the assumption is made that the temperature in the environment falls in the range [59°F, 77°F] or [15°C, 25°C] then in the worst case the measurement of T could be in error by 18°F or 10°C. If this is the case then the graph of dc becomes as Figure 3.2:

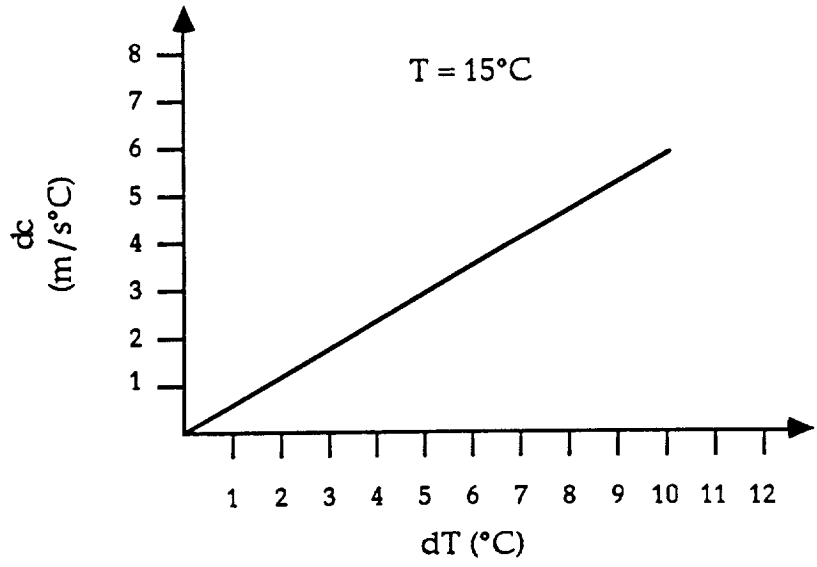

Figure 3.2 — Relation Between dc and dT

Therefore, for

$$dc = \frac{331.18}{546.00} \frac{(273)^{1/2}}{(T + 273)^{1/2}} dT \tag{3.10}$$

with $dT = 10°C$ and $T = 15°C$, for the assumptions given, the maximum value for dc (dc_{max}) ≈ 5.9055 m/s.

Thus the maximum relative error for c is:

$$\frac{dc}{c} = \frac{5.9055 \text{ m/s}}{340.1567 \text{ m/s}} \approx 0.1736 \tag{3.11}$$

and the maximum percentage error for c is:

$$\frac{dc}{c}(100\%) \approx 1.7361\% \text{ error in c} \tag{3.12}$$

Now, to find the error in the slant range measurements, L_i, recall the relationship used to find L_i, namely equation 2.1 which is rewritten here as:

$$L_i = t_i c \tag{3.13}$$

where the distance, D, has been rewritten as the i^{th} slant range, L_i, and the time of flight, t, as the i^{th} time of flight t_i, since each slant range has its own unique time of flight measurement with which it is associated. Further, taking the derivative of 3.13, the change in the i^{th} slant range, dL_i, due to a change in the velocity of sound in the environment can be found as:

$$dL_i = t_i \, dc \tag{3.14}$$

where t_i is treated as an exact constant under the assumption that any equipment that would be used to measure the time of flight would do so with a high enough accuracy so that any error in t_i could be neglected.

Note that a maximum dL (dL_{max}) will occur at a large distance. This is because the time of flight, t, will be greater for a larger distance, and the dc_{max} term as shown above will not change over distance, and therefore will only affect dL as a constant. Now, if the ranges of measurement are limited to distances of L < 3 meters then the time, t_i, will be determined by the equation

$$t_i < \frac{3.0}{c} \tag{3.15}$$

which has a plot of:

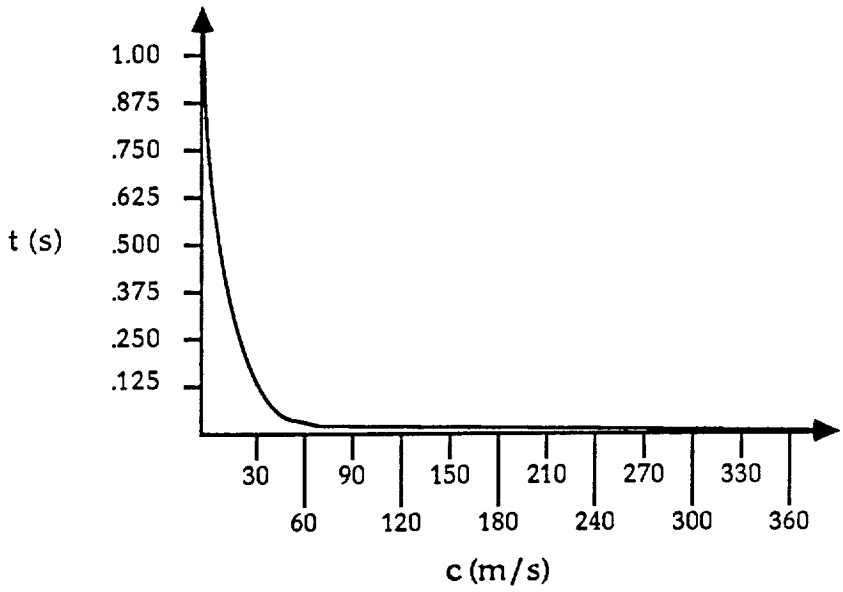

Figure 3.3 — Relation between Time of Flight and Speed of Sound

Note that at the values of c in question — that is from ~340.16 m/s to ~346.01 m/s — the values of t_i in the plot of Figure 3.3 range from ~8.8194 ms to ~8.6703 ms so that the value of t_i acts as a magnitude-reducing scale factor in 3.14. Thus, for the sound velocity range in question $t_{max} \approx 8.8194$ ms.

Now, recalling that the value for dc_{max} occurs when T = 15°C, the maximum dL (dL_{max}) will occur under the same conditions with the time of flight at t_{max}. Thus, if the value of dc in 3.14 is expanded dL becomes

$$dL = t_i \frac{331.18\ m/s}{546°C} \frac{(273)^{1/2}}{(T+273)^{1/2}} dT \tag{3.16}$$

and replacing t_i with t_{max} and dc with dc_{max} as given above gives dL_{max} as:

$$dL_{max} \approx (0.008819\ s)\ (5.9055\ m/s) \tag{3.17}$$

so,

$$dL_{max} \approx 0.05208\ m$$

Thus, the maximum relative error in L is:

$$\frac{dL}{L} = \frac{0.05208\ m}{3\ m} \approx 0.01736 \tag{3.18}$$

and the maximum percentage error in L is:

$$\frac{dL}{L}(100\%) \approx 1.7361\%\ \text{error in L} \tag{3.19}$$

which is the same percentage error for c, and is not surprising since 3.14 shows that dL is related to dc by a constant time value.

Values for dL and the corresponding percentage errors for a distance of L = 3 meters at given temperatures of 15°C, 20°C, and 25°C are given in Table 3.1. Note that as the temperature changes in increments of 0.5°C, dL changes in a linear fashion as predicted by 3.16. It can be seen that for every 1°C change in temperature, the calculated error in the distance measurement will be, at most, approximately 0.1736% of the true distance. Thus, for example, at

a temperature of 20°C over a distance of 1 meter with a temperature change over that distance of 1°C, the measurement error should be approximately 0.1721 cm, or 1.721 mm.

	T = 15°C		T = 20°C		T = 25°C	
dT (°C)	dL	% error	dL	% error	dL	% error
0.0	0.0000	0.0000%	0.0000	0.0000%	0.0000	0.0000%
0.5	0.0026	0.0868%	0.0026	0.0861%	0.0026	0.0853%
1.0	0.0052	0.1736%	0.0052	0.1721%	0.0051	0.1707%
1.5	0.0078	0.2604%	0.0077	0.2582%	0.0077	0.2560%
2.0	0.0104	0.3472%	0.0103	0.3442%	0.0102	0.3413%
2.5	0.0130	0.4340%	0.0129	0.4303%	0.0128	0.4267%
3.0	0.0156	0.5208%	0.0155	0.5164%	0.0154	0.5120%
3.5	0.0182	0.6076%	0.0181	0.6024%	0.0179	0.5974%
4.0	0.0208	0.6944%	0.0207	0.6885%	0.0205	0.6827%
4.5	0.0234	0.7812%	0.0232	0.7746%	0.0230	0.7680%
5.0	0.0260	0.8681%	0.0258	0.8606%	0.0256	0.8534%
5.5	0.0286	0.9549%	0.0284	0.9467%	0.0282	0.9387%
6.0	0.0312	1.0417%	0.0310	1.0327%	0.0307	1.0240%
6.5	0.0339	1.1285%	0.0336	1.1188%	0.0333	1.1094%
7.0	0.0365	1.2153%	0.0361	1.2049%	0.0358	1.1947%
7.5	0.0391	1.3021%	0.0387	1.2909%	0.0384	1.2800%
8.0	0.0417	1.3889%	0.0413	1.3770%	0.0410	1.3654%
8.5	0.0443	1.4757%	0.0439	1.4630%	0.0435	1.4507%
9.0	0.0469	1.5625%	0.0465	1.5491%	0.0461	1.5361%
9.5	0.0495	1.6493%	0.0491	1.6352%	0.0486	1.6214%
10.0	0.0521	1.7361%	0.0516	1.7212%	0.0512	1.7067%

Table 3.1 — Relation Between dT and dL Showing the % Error in L

The preceding results for error in the slant range can be extended to find the errors in the distance measurements required by the problem solution. Recalling the equation for D_X from 3.3 ∂D_X is found as:

$$\partial D_X = \frac{L_2\, dL_2 - L_3\, dL_3}{d_{23}} \tag{3.20}$$

which, after inserting expanded terms for dL_2 and dL_3, and simplifying the result, becomes:

$$\partial D_X = (0.6065) \frac{(273)^{1/2}}{(T + 273)^{1/2}} dT \frac{L_2t_2 - L_3t_3}{d_{23}} \quad (3.21)$$

Taking the derivatives of equations 3.6 and 3.7 yield equations similar to 3.21:

$$\partial D_Y = (0.6065) \frac{(273)^{1/2}}{(T + 273)^{1/2}} dT \frac{L_1t_1 - L_2t_2}{d_{12}} \quad (3.22)$$

and

$$\partial D_Z = (0.6065) \frac{(273)^{1/2}}{(T + 273)^{1/2}} dT \frac{L_2t_2 - L_4t_4}{d_{24}} \quad (3.23)$$

Note that in this case, the error in each of the distances D_X, D_Y, and D_Z depends solely on the error in the temperature measurement. Thus, again using the values T = 15°C and dT = 10°C, as before, the following maximum errors arise in the distance measurements:

$$\partial D_X = (5.9055) \frac{L_2t_2 - L_3t_3}{d_{23}} \quad (3.24)$$

$$\partial D_Y = (5.9055) \frac{L_1t_1 - L_2t_2}{d_{12}} \quad (3.25)$$

and

$$\partial D_Z = (5.9055) \frac{L_2t_2 - L_4t_4}{d_{24}} \quad (3.26)$$

∂D_X, ∂D_Y, and ∂D_Z are maximized when the right hand side of each of their equations is maximized. Again, limiting the maximum measured

distances to 3 meters, and setting $d_{23} = d_{12} = d_{24} = 1$, the maximum values are found to be:

$$\partial D_X = \partial D_Y = \partial D_Z = (5.9055)\,(0.01411) \approx 0.08333 \text{ m} \qquad (3.27)$$

and the maximum percentage errors in D_X, D_Y, and D_Z to be:

$$\frac{\partial D_X}{D_X}\,(100\%) = \frac{\partial D_Y}{D_Y}\,(100\%) = \frac{\partial D_Z}{D_Z}\,(100\%) \approx 2.8735\% \text{ error} \qquad (3.28)$$

Reducing Slant Range Measurement Errors

It has been shown that the measurement accuracy of the slant ranges is most affected by changes in temperature along the flight path of the ultrasonic wave front. Therefore, the method to reduce error in the slant range measurements must be able to determine the temperature changes along the flight path and apply those changes to the known speed of sound. Unfortunately, detecting such temperature changes is a difficult task and therefore requires an attempt to find a simpler method.

Recall that changes in an environment's temperature directly change the speed of sound within that environment. This being the case, if the speed of sound can be accurately measured dynamically (while slant range measurements are being taken) instead of defining it to be a static value for the environment, then the effects of any temperature changes can be applied to the next set of slant range measurements. A simple method of determining the speed of sound is to set up another ultrasound transmitter and receiver unit at a known distance and then measure the speed of sound over that known distance by solving for c from equation 2.1 since D and t are

known; thus, c = D/t. If this calibration measurement is made just prior to measuring the slant ranges then the dynamically measured speed of sound can be used to measure the slant ranges more accurately than if a statically defined speed of sound is used.

This method for dynamically measuring the speed of sound has a drawback in that it gives a measure of c in only one dimension. If the speed of sound can be accurately measured in more dimensions, then the individual speed of sound values can be averaged to find an increasingly accurate value for c. If, for example, two receiver units are used instead of one for the calibration measurement then the value for c can be found as the average of two individual measures of c (c_1 and c_2) and thus take into account fluctuations in temperature over two dimensions:

$$c = \frac{c_1 + c_2}{2} \tag{3.29}$$

An ideal setup for the calibration receivers is to use one receiver, R_1, to measure the horizontal component of the speed of sound (c_1 for example) and the other receiver, R_2, to measure the vertical component of the speed of sound (c_2) as shown in Figure 3.4a.

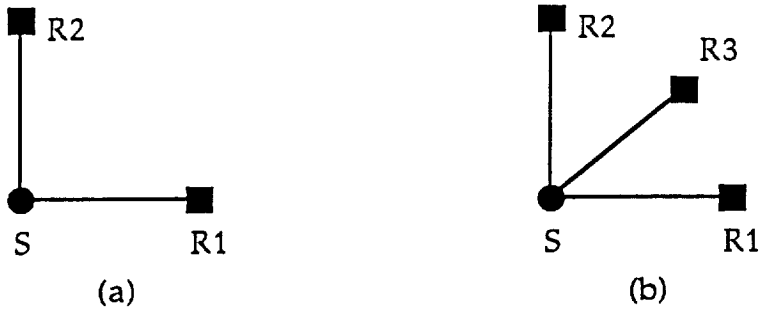

Figure 3.4 — Setup to Calibrate Speed of Sound Value in 2- and 3-Space

Since the two receivers are positioned at right angles, setup (a) takes into account changes in the speed of sound over two dimensions. To include the changes in the speed of sound over the third dimension, a third receiver, R_3, can be added orthogonally to the first two as shown in Figure 3.4b. This additional receiver adds another term to 3.29 to give 3.30.

$$c = \frac{c_1 + c_2 + c_3}{3} \tag{3.30}$$

Therefore, the third term allows fluctuations in temperature over a third dimension to be taken into account. When averaged with the c_1 and c_2 values from the first two dimensions, the c_3 value allows determination of the value of c over the entire 3-space environment.

CHAPTER 4
EXPERIMENTAL RESULTS

Description of Experiment

A foremost concern associated with making ultrasonic time of flight distance measurements is the accuracy of the results based on temperature fluctuations along the path of the ultrasound wave. The more unstable the temperature along the path of flight for the ultrasonic wave front, the more inaccurate the distance measurements will be. The previous chapter demonstrates that the maximum expected percentage error in distance measurements is approximately 1.7361% at T = 15°C and dT = 10°C.

In order to determine the amount of measurement error which might be encountered under lab conditions, a set of distance measurement samples is found for a known distance. The sample mean is calculated from the samples and then used to determine the average measurement error from the data. Additionally, the maximum sample value is used to determine the maximum percentage error in the data. Thus, the average and maximum bounds of measurement error are determined for the sample data.

The experimental setup consists simply of a Polaroid ultrasonic transducer set up at a known distance of approximately 3 meters from a target. The transducer is fired and the distance then calculated from the time of flight of the received target echo. For this experiment, 180 distance measurement samples of the known distance were gathered at the rate of one sample per second to avoid any reverberation errors. The mean was then

determined from the data and used to determine the average percentage measurement error as:

$$\varepsilon_{avg} = \frac{dL}{L}(100\%) \approx \frac{\Delta L}{L}(100\%) \qquad (4.1)$$

where $\Delta L = (L - M)$ with M as the sample mean of the data and L = 3m. Additionally, the maximum percentage error from the data was determined by replacing M with the maximum sampled value for the distance so that ΔL can be rewritten as $\Delta L = (3 - max)$. The magnitude of the percentage error can simply be found by using $|\Delta L|$.

Results of Experiment

From the 180 samples taken, the mean was found to be approximately 3.0016 meters and the maximum sampled value to be 3.007 meters. The calculation of ε_{avg} showed that the magnitude of the average percentage error in the measurement samples was approximately

$$\varepsilon_{avg} = \frac{\Delta L}{L}(100\%) = \frac{|(3 - 3.0016)|}{3}(100\%) \approx 0.0537\% \qquad (4.2)$$

and the magnitude of the maximum percentage error was approximately

$$\varepsilon_{max} = \frac{\Delta L}{L}(100\%) = \frac{|(3 - 3.007)|}{3}(100\%) \approx 0.2333\% \qquad (4.3)$$

The temperature in the room during the time interval in which the sample measurements were taken was approximately 71°F, or 21.6667°C. Consulting the T = 20°C column of Table 3.1 shows that for each of the error

measurements the value of dT over the path of the wave was approximately 0.4°C for the average measured sample, and approximately 1.4°C for the maximum measured sample.

In retrospect, the values for the average and maximum percentage errors seem fairly reasonable, given the temperature of the room and the fairly static temperature conditions therein. Thus, if equipment was set up as in Figure 3.1 to measure the D_X, D_Y, and D_Z 3-space component distance values it would be reasonable to expect that the percentage error values of those components would be considerably less than the predicted maximum percentage error value of 2.8735%.

CHAPTER 5

PROTOTYPE COLLISION AVOIDANCE SYSTEM

Prototype System Design

The problem of avoiding collisions between two independently operating, closely-situated robotic arms can be handled by a two-step process. The first step is the detection of an impending collision and the second is the actual avoidance of the collision. Detection of an impending collision can be handled with the following sequence of steps:

(1) Determine the 3-space locations of important points on the arms (namely the locations of the ultrasound transmitters).

(2) Calculate the distances between the arms using the location of the points found in step 1.

(3) Compare the calculated distances against preselected nearness thresholds to determine if the arms are too close.

(4) Based on the nearness comparison, signal the collision avoidance system if the arms are too close.

The collision avoidance step can be handled by simply taking some evasive action to avoid the collision. The type of evasive action taken could range from simply halting the movement of one or both of the arms to more complicated maneuvering actions to bring the arms to safe distances from each other.

A minimal setup of ultrasound transmitters and receivers necessary for the detection of impending collisions is shown in Figure 5.1. The figure

shows the two robot arms, each with shoulder, elbow, and wrist joints, situated along a rail which allows lateral base movement of both arms.

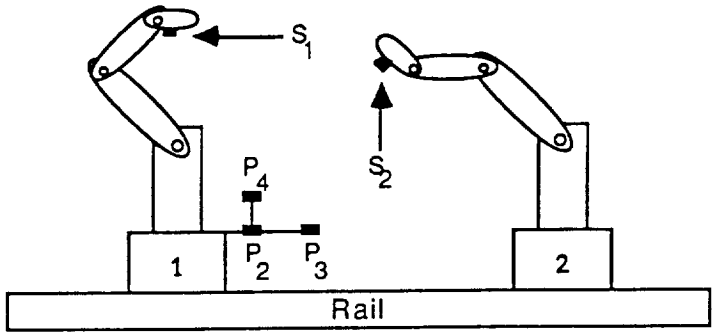

Figure 5.1 — Minimal Setup of Ultrasound Transmitters and Receivers

Connected to the base of arm 1 is the array of the four receivers, P_1 to P_4 (P_1 is not shown as it lies directly behind receiver P_2). The four receivers are set up as discussed in Chapter 3 at distances d_{12}, d_{23}, and d_{24} apart from each other and are used to determine the location of the two ultrasound transmitters (denoted S_1 and S_2) which are connected at the base of each arm's wrist. The transmitters are placed at the bases of the wrists since the assumption is made that each arm's wrist location represents, in general, the maximum extension of the arm into 3-space from its corresponding arm base. Knowledge of the 3-space locations of the wrists from the transmissions of S_1 and S_2 enables the calculation of the distances between them and gives a general estimate of the proximity of the arms. Comparison of the wrists' proximity based on some predetermined nearness thresholds allows the system to determine if a collision between the wrists could occur and therefore whether or not evasive action should be taken.

Prototype System Accuracy

Reducing the total amount of error in the D_X, D_Y, and D_Z measurements is important for the accurate operation of the system. Once the distances between the important points on the arms (the wrists in this simple case) have been calculated, they are compared against nearness thresholds to determine if they fall within a range of distances regarded as too close for safe operation. Inaccuracies in the distance measurements can, therefore, affect the robots in one of two ways. The inaccuracies can trigger the collision avoidance system when the actual distances between the important arm points are not within the range of nearness thresholds, leading to reduced arm movement capabilities. On the other hand, inaccuracies can allow the arms to function even when the actual distances between the important arm points are within the range of nearness thresholds, possibly leading to an undetectable collision.

As previously demonstrated, the percentage error in any of the 3-space component distance measurements should be less than approximately 2.874% with receiver offsets $d_{12} = d_{23} = d_{24} = 1$ meter. However, if offsets of one meter are too large for practical use then their reduction means a reduction in measurement accuracy as shown by equations 3.24 to 3.26. The general form of those equations is given here for convenience.

$$\partial D_A = (5.9055) \frac{L_i t_i - L_j t_j}{d_{ij}} \qquad (5.1)$$

where A is the X, Y, or Z axis and i and j are used to index the slant ranges, time of flights, and offset value. The ratio $5.9055 / d_{ij}$ is simply the ratio of the constant value 5.9055 divided by an offset value d_{ij}. Therefore, if the value

for the offsets is chosen to be less than one meter, it has a multiplicative effect on the error. For this reason, it is advantageous to allow the offset distances between the receivers to be as large as possible.

Additional inaccuracies arise from the use of only two ultrasound transmitters in the original design. Problems can arise because other of the locations on each of the arms, are not able to be determined. It is possible, for example, for the shoulder joint of arm 1 to be closer than the wrist joint of arm 1 to a point on arm 2. If this is the case, then the simple two-transmitter design is limited in its ability to accurately determine if a collision will occur. One method to overcome this limitation is to add additional transmitters at each major joint (shoulder, elbow, and wrist) on each arm so that the locations of these joints can be determined. Since the arms consist of rigid segments of known lengths, a simple point-to-point line algorithm can be used to draw a line segment between every joint on either of the arms so that the full 3-space description of each arm location can be determined. Ultimately, then, the distance between any point on arm 1 to any point on arm 2 can be tested against the nearness thresholds to determine if a collision might occur.

Another concern with the minimal setup of Figure 5.1 arises from the realization that when either arm 1 or 2's transmitter is placed near 180° from the receiver setup the possibility exists that the ultrasound transmissions from S_1 or S_2 will be lost, or only detected after reflection of the transmitted wave occurs. One method of handling a lost transmission is to simply assume that the arm's transmitter is currently facing away from the receivers. Unfortunately, when only one transmitter per arm is used, no method exists for determining if the entire arm is facing away from the receivers, or only

the wrist. If multiple transmitters are utilized on an arm then the detection of none, some, or all of the multiple transmissions allows the collision detection system to determine which parts of the arm are facing away from the receivers (and therefore are not in danger of colliding with the other arm).

Determining whether a transmission is lost inherently requires some type of timeout procedure which takes into account the reverberation time of the transmission in the environment. If timeout is not considered, then the possibility exists of a reverberated transmission either reaching the receivers and being counted erroneously as a valid distance or hanging up the collision detection system indefinitely while the system waits for it to arrive. Knowledge of the reverberation time within a room is necessary, as well, so that the collision detection system can determine the proper time to fire the next ultrasound transmitter so that separate transmissions will not interfere with each other (assuming that each transmitter operates at the same frequency).

The reverberation time of a room can be calculated from the following formula[4]:

$$t_r = \frac{4\,V \ln(I_0 / I)}{8\alpha V - S \ln(1 - a)\, c} \qquad (5.2)$$

where V is the volume of the room in m^3, I_0 / I is the reduction in intensity of sound by 10^6 db, S is the total wall surface of the room in m^2, c is the speed of sound in the room, and α and a are the absorption coefficients of the gaseous medium and room walls respectively.

Using 5.2, t_r can be found for a several different room sizes. If α and a are held constant at $\alpha \approx 0.06$ for air at 20°C (based on classical attenuation at a frequency of about 40 KHz) and $a \approx 0.2$ for average room structure attenuation then a table of reverberation time values can be obtained.

Room Dimensions (m)			Reverberation Time (ms)		
Length	Width	Height	$\alpha = 0.06$	$\alpha = 0.08$	Average
5	5	3	198.99	166.08	182.54
5	10	3	210.64	174.11	192.38
5	15	3	214.83	176.96	195.90
10	10	3	223.73	182.96	203.35
10	15	3	228.46	186.12	207.29
15	15	3	233.41	189.38	211.40

Table 5.1 — Reverberation Time For Rooms of Different Sizes

Table 5.1 demonstrates that in a room heated to 20°C, the time required to pass before a transmission can be considered as lost is approximately 218 ms for $\alpha = 0.06$ and 179 ms for $\alpha = 0.08$. Obviously, if the collision detection system must wait, on average, approximately 198.8 ms for each transmission to die out, it behooves the designer to keep the number of transmitters in the system low so that the time required to find all the necessary arm locations is low. If the time to find all the arm locations is too high, a collision may occur before the system has a chance to determine the locations of all the transmitters.

One workaround to this problem is to use ultrasound transmitters of different frequencies so that all of the transmitter locations can be found in

parallel. The disadvantage with parallelness is that all of the receiver circuitry must be reproduced n times for n transmitters. Additionally, the frequencies to be used for transmitting must not contain overtones which match another transmitting frequency or else ambiguity may occur when determining transmitter locations.

Improving System Design

Based on the considerations presented for reducing the inaccuracies of the two-transmitter system, several improvements can be made to the original prototype design. Clearly, for more accurate arm location determination, additional transmitters are necessary. If another transmitter is placed at the elbow joint of each arm it becomes possible to mathematically determine the location of all points on the arms using the point-to-point line algorithm discussed previously.

The addition of two more transmitters augments the total time necessary to find all the necessary arm locations by twofold. To reduce the total reverberation time, anywhere from one to four distinct transmitting frequencies can be used so that transmission can occur in parallel. This adds to the total cost of the system due to redundant hardware, but reduces the time of reverberation to a more acceptable value.

Finally, improvements in the calibration of the speed of sound can be utilized to reduce errors in the slant range measurements. Calibration of c requires at least one more ultrasound transmitter and receiver and possibly more as previously discussed in Chapter 3. The additional transmitters' reverberation time must be considered, and used to determine how many, if

any, speed of sound calibration transmitters should be used. Clearly, if the total reverberation time for the system is fairly high then the distance measurements will not be gathered often enough to be of any timely use, and the accuracy of the distance measurements will be inconsequential.

CHAPTER 6

CONCLUSIONS

Summary and Conclusions

A method of measuring distances using an ultrasound time of flight measurement method was examined in order to determine the bounds on measurement error due to temperature fluctuations along the path of the ultrasonic wave front. An upper bound on measurement error was determined to be maximally 1.7361% of the distance when a temperature change of 10°C was encountered over the path of the wave front. When applied to the collision detection and avoidance solution presented, this measurement error for slant ranges translates to an overall maximum error of approximately 2.8735% for each of the 3-space location components D_X, D_Y, and D_Z used to determine the 3-space locations of ultrasound transmitters on the robot arms.

The key method presented to minimize the measurement errors suggests that a more exact measurement of the speed of sound can reduce the error. By using multiple ultrasound transmitters and receivers, set up at known distances, a better estimate of the speed of sound can be determined over two or three dimensions. This improved estimate of the current speed of sound in the environment can be used to improve the overall accuracy of the slant range measurements.

Experimental evidence suggests that the distance measurement errors do seem to follow the relationship which states that changes in distance measurements are directly proportional to changes in the temperature along

the path of the ultrasonic wave front. Additional experimental evidence suggests that it is possible to make ultrasound distance measurements within 0.25% of the exact value at common room conditions. This would indeed appear to support the idea that distance measurements made via the ultrasound time-of-flight method are suitable for a basic collision detection and avoidance system.

Suggestions for Further Research

The following list suggests steps which can be taken to further the efforts of the research completed thus far. Further research time spent examining the areas listed below will provide a better understanding of the feasibility of ultrasound to solve the collision avoidance problem.

(1) Construction of a prototype collision avoidance system. This would require the construction of ultrasound transmitting and receiving hardware.

(2) Interface of hardware with robot arms and a computer to control all of the ultrasound transmissions as well as compute the necessary calculations of 3-space location components.

(3) Determination of the 3-space location component (D_X, D_Y, D_Z) errors in the system.

(4) Attempted reduction of errors by speed of sound calibration techniques using additional ultrasound transmitters as discussed in Chapter 3.

(5) Determination of the effects of adding additional transmitters to system to implement point-to-point line segment algorithm discussed in Chapter 5.

(6) Determination of the feasibility of using multiple transmission frequencies for parallel ultrasound transmission as discussed in Chapter 5.

(7) Interface of collision avoidance system with existing control software for robot arms to determine the geometrical and time limits of ability of the system.

(8) Extension of work to an RF domain solution for use in activities where ultrasound is not feasible; use in space for example. Information on one possible technique using Polhemus 3SPACE three-dimensional position and orientation sensors is given in [10] and [11].

Steps 1 through 7 deal with implementing and then improving the accuracy and overall timeout requirements of the ultrasound solution. Conceivably, the implementation of step 8 would entirely eliminate the reliance on time of flight measurements for the current design and thus the effects of timeout discussed in the previous chapter. The parallel monitoring of the locations of the transmitters on the arms would allow for faster determination of the arm positions and, in doing so, possibly yield results suitable for a realtime solution.

CHAPTER 7

LITERATURE CITED

[1] Brown, B., Goodman, J., High-Intensity Ultrasonics. Princeton, NJ: Nostrand, 1965.

[2] Humphreys, W., Physics of the Air. New York, NY: McGraw-Hill, 1940.

[3] Sears, F., Young, H., and Zemansky, M., University Physics. Reading, MA: Addison-Wesley, 1982.

[4] Beyer, R. and Letcher, S., Physical Ultrasonics. New York, NY: Academic, 1969.

[5] Coppens, A., Frey, A., Kinsler, L., and Sanders, J., Fundamentals of Acoustics. New York, NY: Wiley, 1982.

[6] Rossi, M., Acoustics and Electroacoustics. Norwood, MA: Artech House, 1986.

[7] Beranek, L., Acoustic Measurements. New York, NY: Wiley, 1949.

[8] Lindsay, R., Physical Acoustics. Stroudsburg, PA: Dowden, Hutchinson & Ross, 1974.

[9] ɛl' Piner, I., Ultrasound: Physical, Chemical, and Biological Effects. New York, NY: Consultants Bureau, 1964.

[10] Foley, J., van Dam, A., Feiner, S., and Hughes, J., Computer Graphics: Principles and Practice, Second Edition. Reading, MA: Addison Wesley, 1990, 355.

[11] Zimmerman, T., Lanier, J., Blanchard, C., Bryson, S., and Harvill, Y., "A Hand Gesture Interface Device," Proceedings of the CHI and GI 1987 Conference, New York, NY: ACM, 1987, 189-192.